

Particle Astrophysics

John Carr*

*Centre de Physique de Particules de Marseille, 163 Avenue de Luminy, Case 907, 13288
Marseille, France. E-mail: carr@cppm.in2p3.fr*

ABSTRACT: This review covers recent developments in Particle Astrophysics in two areas: High Energy Astronomy and Dark Matter Searches. The sources of high energy cosmic rays are still largely unknown but new data is becoming available which could clarify the situation. Recent measurements of cosmic ray anisotropy and mass composition are presented together with results from high energy gamma and neutrino detection. Advances in detectors in these fields are reviewed. New results are discussed on searches for dark matter in the form of both baryonic and cold dark matter.

1. Particle Acceleration in Astronomical Sources

It is generally believed that the bulk of cosmic rays in the energy range 10^9 to 10^{19} eV, observed on Earth, are accelerated in the shock wave of matter ejected in violent phenomena in astronomic objects. Among the astronomic objects capable of high energy acceleration are supernova remnants where the shell of matter expands at a significant fraction of the speed of light and quasars/microquasars where the matter in the jets moves relativistically with Lorentz boosts of 10 or higher. Calculations of charged particle acceleration in shock waves originated with Fermi and involve stochastic elastic collisions of the particles with the moving matter giving an average energy gain to the particle. This process can be very efficient, for example calculations of Berezhko and Volk [1] predict up to 50% of the energy in the ejected matter of certain supernova remnants can be converted to cosmic rays after timescales of the order of 1000 years after the supernova explosion.

While it is well known that protons and heavy ions dominate the flux of cosmic rays arriving on Earth, there is controversy as regards the nature of the major component of the accelerated particles in some sources. The observed spectra of x-rays and gamma rays from Active Galactic Nuclei can be explained in some models [2] invoking solely the presence of high energy electrons in the source. Other models [3], however, succeed in explaining the features of the spectra using proton acceleration. Experiments could distinguish between these different models by searching for neutrinos coming from the sources. Neutrinos would

*Speaker.

be emitted in the decay of pions in hadronic showers produced by proton interactions in the matter or radiation field surrounding the source, while in the dominant electromagnetic processes following electron acceleration, few hadrons and neutrinos would be generated

2. Sources of High Energy Particles

The origin of the bulk of the high-energy cosmic rays observed on Earth is at present largely unknown. The measured features of the spectrum of the charged cosmic rays, shown in figure 1, will be described in section 4. It is expected that the majority of cosmic rays with energies below about 10^{18} eV have their origin in our own galaxy while those at higher energies come from extragalactic sources. As will be described in section 8, high-energy gamma rays have been observed from numerous sources and it would be natural to expect charged cosmic rays also to originate from these. The uncertainty mentioned in the previous section as to the nature of the accelerated particles being either hadrons or electrons, however, means that it is not clear that the sources observed on Earth with different probes will be the same; this then is a motivation for multi-messenger astronomy at high energies.

In the galaxy it is Supernova Remnants (SNR) which are most popularly predicted to be the source of charged cosmic rays. A supernova remnant comprises a shell of matter, emitted after a supernova explosion, which continues to expand at speeds of typically a few tenths of the speed of light for thousands of years. The catalogue of Green lists over two hundred galactic supernova remnants of which several correspond to optically observed supernova (SN). A handful of SNR's have central pulsars and are known as plerions; the most famous being the Crab Nebula (SN1054). Some of these sources are known to be powerful emitters of TeV

gamma rays but shell SNR, without a central pulsar, are less easily visible in TeV gammas.

Active Galactic Nuclei (AGN) are also known sources of TeV gamma rays. These objects, where jets of matter are emitted from the galaxy nucleus, are possibly a stage in the evolution of the majority of galaxies. The distribution of AGN's peaks at red shifts around 2, distances around 10 Gpcs, with the closest observed in TeV gamma around 100 Mpcs.

Microquasars are thought to have the structure of a small scale AGN. Since 1992 about a dozen microquasars have been observed in the galaxy [4]. Multi wavelength observations support the model of microquasars as black holes of a few solar masses surrounded by

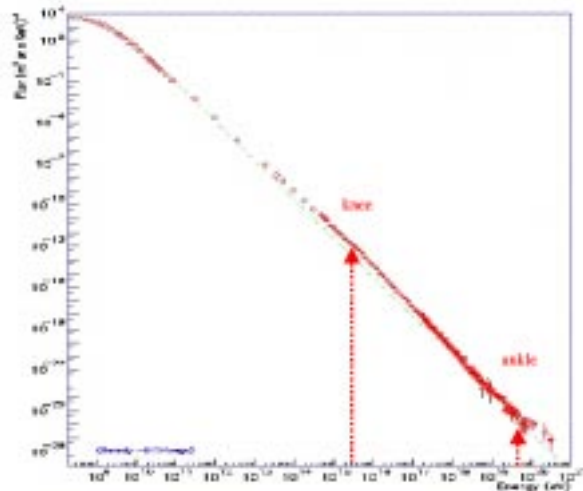


Figure 1: Compilation of Cosmic Ray Data, illustrating 'knee' and 'ankle' features.

an accretion disk fed from a companion star. The episodes of emission of high energy radiation, seen as separating blobs in radio telescope images, are explained as being due to instabilities in the accretion disk where the inner few hundred kilometres of material falls into the central black hole, with some fraction of this material being ejected in back-to-back jets.

Gamma Ray Bursts (GRB) are energetic sources observed to emit short bursts of gamma's in the energy range of a few hundred MeV with burst durations between 100ms and 100s. When it was operational the BATSE detector on the Compton Gamma Ray Observatory observed 1-2 events per day. The distribution of the BATSE observed GRB's, is uniform in galactic co-ordinates giving an indication of extragalactic origin. For about 20 GRB's with long burst duration, the redshift of the after glow has been observed and all are measured to be extragalactic. Many theories exist for the nature of gamma ray bursts and more data is needed to distinguish between them.

3. Instruments for High Energy Astronomy

The existing data on cosmic rays comes from numerous detectors. In the low energy range, below about 10^{13} eV, the flux of primary cosmic rays must be measured above the atmosphere in satellites and balloons to avoid interactions in the air. At higher energies, 10^{13} - 10^{20} eV, the showers in the atmosphere can be observed from the ground with telescopes sensitive to the fluorescence and Cherenkov light produced or from the particles arriving at the surface with extensive air shower arrays. Among the active extensive air shower arrays currently producing results are the AGASA [5] detector in Japan and the KASCADE [6] detector in Germany. A complete review of ultra high-energy cosmic ray detection techniques and data can be found in [7].

As for charged cosmic rays, at low energies the primary gamma rays are observed above the atmosphere with detectors such as those on the Compton Gamma Ray Observatory, BATSE and EGRET, where the energy range was up to 10^9 eV. The existing ground based gamma ray telescopes are of two basic sorts: in the range around $\sim 10^{12}$ - 10^{14} eV telescopes such as WHIPPLE [8] and HEGRA [9] and in the intermediate energy range $\sim 10^{10}$ - 10^{12} eV recycled thermal solar arrays such as CELESTE [10] and STACEE [11].

There are currently two operating neutrino telescopes: BAIKAL [12] at a depth of 1200 m in the water of Lake Baikal in Siberia and AMANDA [13] at a depth of 2000 m in the ice at the South Pole in Antarctica. These detectors are sensitive in the energy range $\sim 10^{10}$ - 10^{15} eV.

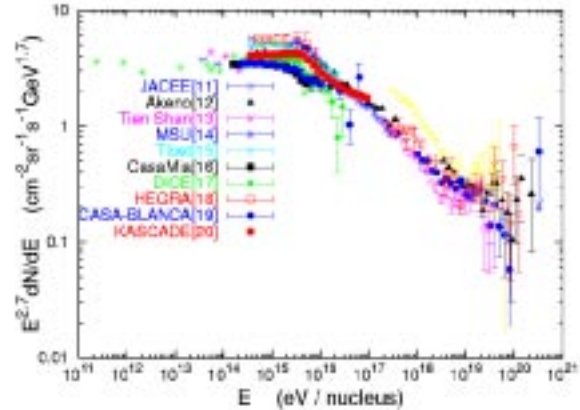


Figure 2: High Energy Cosmic Ray Data, plotted as flux times $E^{2.7}$ to accentuate the knee feature [17].

4. Cosmic Ray Spectrum

Figure 1 shows a compilation of cosmic ray data made by Swordy [14]. The features of this spectrum are a differential flux $dN/dE \propto E^{-2.7}$ for energies between 10^{10} and 10^{15} eV which changes in slope around $\sim 4 \cdot 10^{15}$ eV at the so-called 'knee', to a flux $dN/dE \propto E^{-3.2}$ for energies between 10^{16} to 10^{18} eV. Around 10^{19} eV there is another change in slope, the 'ankle', and the flux becomes approximately $dN/dE \propto E^{-2.8}$. The details of the knee and ankle are better seen in figure 2 where the flux is multiplied by $E^{2.7}$ to make the distribution flat in the lower part of the plot. The cause of these slope changes at the knee and ankle are not known and are the subject of much speculation.

Models of particle acceleration in shock waves typically give fluxes at the source $\propto E^{-(2.0/2.2)}$ and transport calculations through the galaxy taking into account diffusion can soften this spectrum to that observed $\propto E^{-2.7}$. In some models the change to $\propto E^{-3.2}$ above $4 \cdot 10^{15}$ eV comes from losses due to non-confinement in the galactic magnetic field, however it does not seem natural that such a mechanism would give the sharp knee apparent in figure 2. The hardening of the spectrum above 10^{19} eV could be due to the increasing dominance of the extragalactic flux over the galactic flux. Above 10^{20} eV there are indications of different, possibly exotic, contributions since charged cosmic rays above this energy from distant sources will be attenuated due to interactions on the Cosmic Microwave Background Radiation of 2.7K photons: the GZK cut-off [15]. Figure 3 shows the flux expected at Earth from a distribution of sources uniform throughout the universe, taking into account the GZK effect, compared with the observed ultra high-energy cosmic ray data [16]. The data clearly extends beyond the curve indicating inaccuracies in the assumptions of the calculation and so something to be understood.

One explanation of the knee structure, which is attractive but lacking experimental evidence, is that of a single dominate source possibly a single close SNR [18]. This can explain the sharpness of the slope change as due to the energy limit of the particular source acceleration. Acceleration limits in multiple sources are unlikely to be at a fixed energy due to differences in the parameters of the source such as size, magnetic field and density, hence the need for the single source. The problem with this idea is that the identity of this source is not apparent. It is natural that it would be observable in gamma rays and neutrinos as a localised source while in charged cosmic rays the galactic field would mask

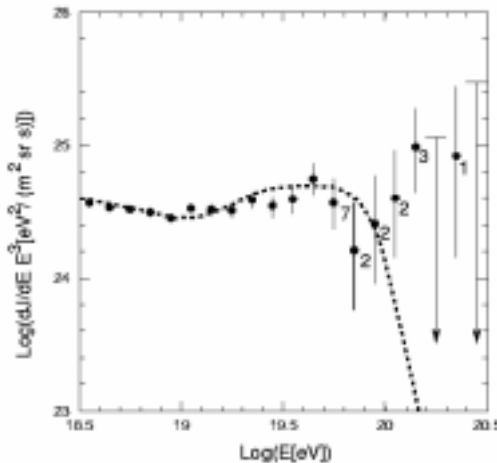


Figure 3: Ultra high-energy cosmic ray data plotted as flux time E^3 demonstrating the ankle feature. The curve indicates the spectrum which would be expected for sources having a uniform distribution throughout the universe.

all directional information. Among other explanations, is the absorption of cosmic rays on a field of massive neutrinos causing a cut-off above a certain energy. In the version of this model due to Wigmans [19], it is an interaction with electron neutrinos with a mass of 0.1eV giving a threshold in the interaction $p + \nu_e \rightarrow n + e$, while in the model of Dova et al. [20] the reaction is $p + \nu_\mu \rightarrow \Delta + \nu_\mu$, where the ν_μ is given a mass of 100eV to arrange the necessary threshold. To give high enough interaction rates to explain the data these models need either clumps of neutrinos with high density or neutrino magnetic moments.

For the ultra high energy cosmic rays (UHECR) with energies above $\sim 10^{20}$ eV, there are two classes of explanations: “bottom-up” where the particles are accelerated in sources to be determined and “top-down” where the particles observed are the decay products of massive entities. The difficulty of finding sources capable of acceleration beyond 10^{20} eV has been discussed by many authors eg. [21]. In order to confine particles for a time long enough for the acceleration to occur, the product of source size and magnetic field must be large, however analysis of possible sources types indicates that while some objects have large fields and others large sizes few have both. To avoid the GZK cut-off the sources should be closer than 100 Mpc and there are few likely candidates at this distance scale. In addition, if the sources are close and few, the directions of the observed UHECR should point to them. The data on this issue is described in section 6, but does not correspond to obvious candidates. Among the top-down scenarios are the decays of super-massive particles such as the X particles in Grand Unified Theories and Topological Defects [22].

5. Mass composition of Cosmic Rays

Clear knowledge of the composition of cosmic rays in terms of particle type or mass, would help in distinguishing between the many explanations of their origins. In space based experiments spectrometers can be used to separate the particle types, however for ground based detectors the separation is more difficult. Some ground experiments measure the particle content of the showers reaching the surface to estimate the nature of the primary cosmic ray while others measure the average depth in the atmosphere of the primary interactions.

The KASCADE collaboration showed new data at this conference on the mass composition for cosmic rays with energies around the knee region [23]. The data shown in figure 4 indicates that the slope change in the differential flux spectrum is at progressively higher

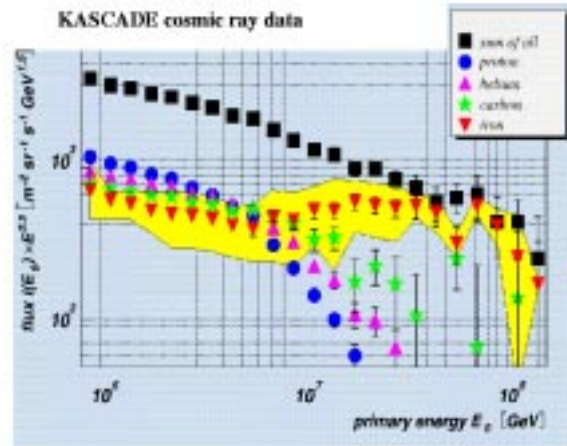


Figure 4: Cosmic ray energy spectra from the KASCADE experiment for different nuclei.

energies for primary cosmic ray nuclei with increasing mass. This progression is such that the knee energy $E(\text{knee}) \propto Z$, the charge of the nucleus. If confirmed, this result seems to be a strong indication that the knee is due to the confinement limit in acceleration where it would be expected that $E(\text{max.}) \propto Z B R$, where B and R are respectively the magnetic field and size of the source.

6. Anisotropy of Cosmic Rays

Only charged cosmic rays of the highest energies can arrive at the Earth after crossing the magnetic field in the galaxy and retain any directional information from the source; protons of energies of 10^{19}eV would be deviated by about 10° in crossing the thickness of the galaxy.

Data from the extensive air shower arrays has been analysed to search for structure in the distribution of cosmic rays above 10^{19}eV . Figure 5 shows the distribution in the sky for events with energies greater than $4 \cdot 10^{19}\text{eV}$ from the AGASA array [24]. In this data there is some evidence of clustering of events; in the events above 10^{19}eV there are pairs and triplets of events which coincide in direction within a cone of 2.5° . The chance probability that this distribution would arise in a uniform random sample is less than 1%. An analysis [25] has combined data from all the experiments yielding a chance probability

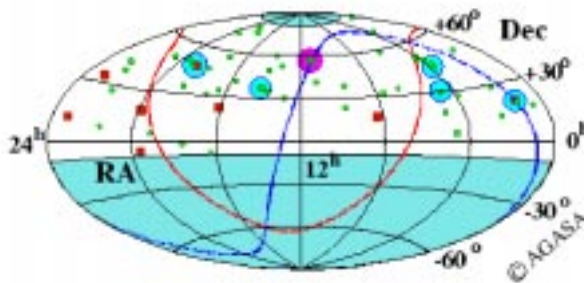


Figure 5: Data from AGASA showing the arrival directions of cosmic rays with energies above $4 \cdot 10^{19}\text{eV}$. Red squares and green circles represent cosmic rays with energies greater than 10^{20}eV , and $(4 - 10) \cdot 10^{19}\text{eV}$, respectively. Shaded circles indicate event clustering within 2.5° .

from all the data which is similar to that from the AGASA data alone. A number of attempts have been made to correlate the locations of these concentrations of events with astronomical objects, but no such association has been clearly demonstrated.

In the AGASA data there is an intriguing concentration of events near, but not exactly at, the galactic centre in the energy range $8 \cdot 10^{17}$ to $8 \cdot 10^{18}\text{eV}$ [26]. A similar concentration of events is seen in data from the SUGAR experiment [27], although the effect is in fact several degrees away from position of the AGASA effect and not compatible with the same point given the experimental resolutions. Figure 6 shows this data. Charged cosmic rays originating from a point source near the galactic centre would be diffused and appear at the Earth spread over a much larger angular region than that seen in the data and reference [27] suggests the effect is in fact due to a flux of neutrons from a source near the galactic centre, which at these energies can travel to the Earth without decaying. Further data is needed to understand if this effect is real but charged cosmic ray data expected in the coming years may not have a significant impact on the situation due to the energy range of

the new experiments. Data from a future neutrino telescope in the Northern Hemisphere could help to resolve the issue.

7. Future cosmic ray experiments

The year 2001 saw the operation of the first elements of the new extensive air shower array, AUGER [28]. This project, with the first site in the southern hemisphere in Argentina, comprises an array of 3000 water Cherenkov tanks covering a surface area of 3000 km² and sets of fluorescence telescopes at four sites throughout the array. The 'engineering array' of this project consisting of 40 tanks and one set of telescopes was deployed between Feb. 2000 and Apr. 2001, giving the first data in May 2001. The southern site is planned to be finished in 2004 with the possibility of finishing the northern site in Utah by 2007 if funding is available.

Among new space cosmic ray experiments is the AMS project [29]. The first version of this experiment flew in the space shuttle in June 1998. The data from this flight has been used to set a limit on the anti-helium/ helium ratio in cosmic rays at 10^{-6} . An upgraded detector is currently being constructed with the intention of installation in the International Space Station in 2004. This detector will for the first time make use of a superconducting magnet in space which will extend the measurement capabilities of AMS towards particle energies of a few TeV.

8. Gamma Ray Astronomy

Since its origins in the 1960's, gamma ray astronomy has made use of space based detectors for low energies and ground based detectors for higher energies, in a similar way to cosmic ray observations. For gamma rays, however, there is not complete energy range coverage at the present time. The ground-based telescopes have over the years built up observations of sources in the TeV range, which have sometimes seen inconsistencies between different data sets.

Tables 1 and 2 show a recent compilation of observed sources from different telescopes [30], containing a quality factor for the confirmation of the observations. In the galaxy there are two well confirmed sources, the Crab and PSR 1706-44, both supernova remnants with

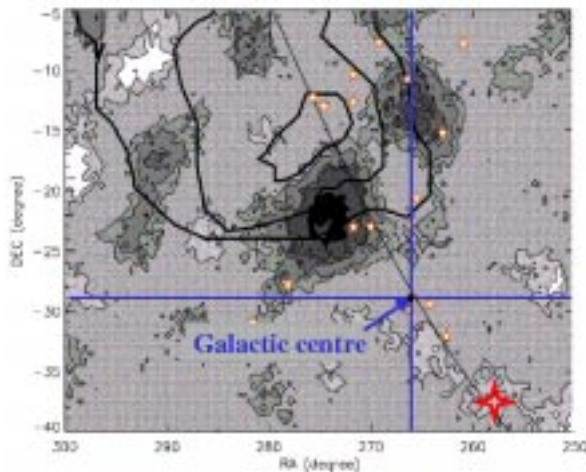


Figure 6: Cosmic Ray Data from AGASA and SUGAR in the energy range near 10^{18} eV indicating an enhancement of cosmic rays from near (but not exactly at) the galactic centre. The shaded contours indicate levels of excess above background in the SUGAR data and the thick contours are the excess in the AGASA data. Positions of known sources of GeV and TeV gamma rays are plotted as stars.

Source name	Source type	discovery date	quality code
Crab	SNR Plerion	1989	A
PSR 1706-44	SNR Plerion ?	1995	A
Vela	SNR Plerion	1997	B
SN1006	SNR Shell	1999	B-
RXJ1713-3946	SNR Shell	1999	B
Cassiopeia A	SNR Shell	1999	B
Centaurus X-3	Accreting Binary	1999	C

Table 1: Galactic sources observed in TeV gamma rays, see [30] for quality code definition.

Source name	Source type	discovery date	quality code
Markarian 421	XBL	1992	A
Markarian 501	XBL	1995	A
1ES 2344+514	XBL	1997	B
1ES 1959+650	XBL	1999	B-
BL Lac	RBL ?	2001	C
PKS 2155-3044	XBL	1999	B-
1H 1426-428	XBL	2000	B
3C66A	RBL	1998	C-

Table 2: Extragalactic sources observed in TeV gamma rays, see [30] for quality code definition.

central pulsars and in the extragalactic sources there are two well confirmed AGN's, Mrk 421 and Mrk 501. Many observations of shell supernova remnants have been made in order to test the hypothesis that these are the sources of galactic cosmic rays, however only three such objects have been seen in TeV gamma rays and these data need independent confirmation. The flux of gamma rays from AGN's is extremely time dependent, being dominated by flares. In some cases the sources can only be observed during flaring periods and most likely some of the discrepancies in source observations can be explained by different telescopes observing at different periods. Data was shown at the conference from the HEGRA collaboration showing flares from Mkn 421 with flare timescales variations of the order of hours [31], indicating that the emission region must have solar system dimensions or smaller. The energy spectrum in the HEGRA data of a Mkn 421 flare in 2001 extends to greater than 10 TeV and has been used to give a limit on the flux of infrared photons, in the intervening space, on which high-energy gamma rays will be absorbed. This limit is less than previous measurements and the discrepancy is not understood [32].

9. New Gamma Ray Telescopes

The imaging Cherenkov gamma ray telescopes only have a small angular acceptance and must target particular sources individually. The choice of viewing field must follow other prior observations and hence provides a bias in the types of observations made.

The MILAGRO project [33] avoids this problem with a large solid angle detector which is an air shower array using a pool of water with photo-detectors at two levels to distinguish gamma induced showers from the dominant rate of hadron induced showers. A small version of the detector, MILAGRITO, has been running for some years and has published observations of the CRAB, Mkn 501 and some evidence for the detection of the gamma ray burst, GRB 970417a [34]. Recently the full scale MILAGRO detector has become operational. The latest observations give no further evidence for coincidences of TeV gamma rays with gamma ray bursts observed at lower energies [35].

In the field of ground based telescopes there are three new projects: Veritas and MAGIC in the Northern Hemisphere and H.E.S.S. in the Southern Hemisphere. H.E.S.S. will greatly increase the scope of TeV gamma measurements in the southern sky and both H.E.S.S. and MAGIC should start operating in 2002.

10. Neutrino Telescope Projects

Among the Neutrino Telescope projects, the largest operational detector is the ice Cherenkov detector, AMANDA II, in Antarctica at the South Pole. The only functional large water Cherenkov detector is the BAIKAL NT200 in Lake Baikal. Limits on high-energy neutrino fluxes have been shown recently from both these experiments. The underground experiment MACRO [36] has also published results.

Figure 7 shows the recent limits from BAIKAL [37] and AMANDA [38], [39] on the diffuse flux of neutrinos. These limits start to be close to some model predictions [40] of fluxes of neutrinos from AGNs but are still an order of magnitude higher than some theoretical limits based on cosmic ray fluxes [41].

The AMANDA experiment has limits on point source fluxes using their data from 1997 [39]. This data limits the flux from objects in the northern visible sky to less than $10^{-7} \text{cm}^{-2} \text{sec}^{-1}$ at 90% confidence level.

Since the 1997 data taking period, AMANDA has increased the size of the detector and improved the signal readout technology. The AMANDA B10 detector had 10 strings and the present AMANDA II detector has 19. The signal readout on the new strings is performed by optical fibre links while the earlier strings have readout on twisted pair cables. The rise time of the signal pulses read out by the analogue optical links is improved to 7ns compared to that of 100ns on the twisted pair readout. The net result of the changes to

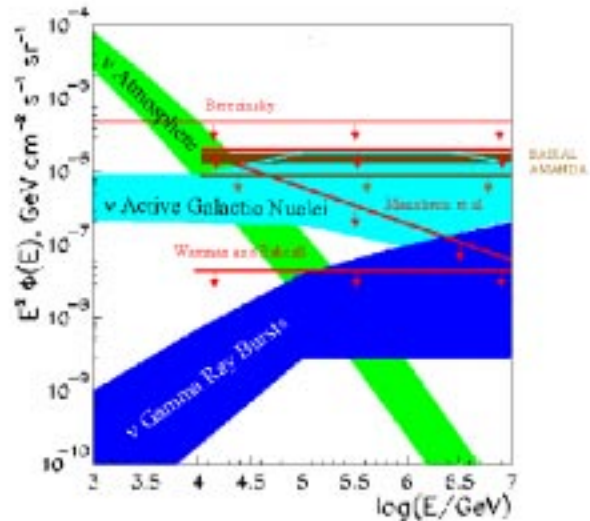


Figure 7: Limits on a diffuse flux of high energy neutrinos from the BAIKAL and AMANDA experiments. Theoretical limits from Berezinsky, Mannheim et al. and Waxman and Bahcall; the flux from atmospheric neutrinos and the range of fluxes of neutrinos from Active Galactic Nuclei and Gamma Ray Bursts from various models are shown.

the AMANDA detector give a detected event rate increased by a factor 4 to 5, together with a very much larger angular acceptance [42].

11. Future developments in neutrino astronomy

The proposal for a future large neutrino detector at the South Pole, Icecube, has recently received a favourable opinion from the US funding agency and government. The detector will consist of 80 strings with a total of 4800 optical modules. The detector will have an instrumented volume of about 1 km^3 with a threshold of $0.5 - 1.10^{12} \text{ eV}$. Construction could start in 2003 with the completed detector expected around 2010.

For Northern Hemisphere neutrino water Cherenkov detectors there are a number of projects. The BAIKAL group intends to increase significantly the size of their detector for very high energy ν_e by adding three outrigger strings. The ANTARES [43] collaboration, after a phase of research and development, is now engaged in the construction of a detector with effective detection area of about 0.1 km^2 . The site chosen for this detector, which will consist of ~ 1000 optical modules, is in the Mediterranean Sea offshore from Toulon in France. This phase of the project should be complete in 2004 and will lead towards a future 1 km^3 project at a site to be determined in the Mediterranean. The NESTOR [44] collaboration plans to deploy a detector consisting of 168 optical modules in a tower structure in 2003.

Northern Hemisphere neutrino detectors will complement the sky coverage of the South Pole detectors as indicated in figure 8, where the region of the sky observed is plotted on a sky map showing gamma ray data. With the assumption given in the figure caption, a detector at the South Pole observes half the sky all the time, while a detector at 43° north, such as ANTARES, observes part of the sky all the time and part of the sky a fraction of the time. The Northern and Southern detectors together observe all the sky with a significant overlap, however only the Northern detector can observe the centre of the galaxy and the majority of the galaxy disk.

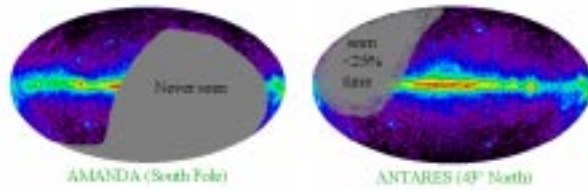


Figure 8: Region of the sky in galactic co-ordinates observed by neutrino telescopes, AMANDA and ANTARES. The visible regions are illustrated on a background of the diffuse gamma ray flux observed by EGRET to indicate the position of the galaxy. The visible regions are drawn with the assumption that the neutrino telescopes have 100% efficiency in the complete downward hemisphere.

12. Dark Matter

The present knowledge of the composition of matter in the universe comes from observations of galaxy clusters, cosmic microwave background radiation, Supernovae type 1a and big bang nucleosynthesis. In the current picture [45], the total amount of matter is close to the critical density for a flat universe with $\Omega_{total} \sim 1$ and the fraction of matter is

30% with the rest being the, as yet, little understood 'dark energy'. The matter contribution consists of baryonic matter with $\Omega_b \sim 0.04$ and cold dark matter with $\Omega_{\text{CDM}} \sim 0.26$. A detailed review of searches for dark matter is given by L. Bergstrom in reference [46].

13. Baryonic dark matter searches

Only a small fraction, $\Omega \sim 0.004$, of total matter is explainable by luminous stars compared to the $\Omega \sim 0.04$ baryonic matter expected from big bang nucleosynthesis, hence a substantial fraction of baryonic matter must be dark. A number of searches have been made for a contribution to this baryonic dark matter in the form of brown dwarfs: stellar like objects with insufficient mass to burn hydrogen. These searches observe fields of distant luminous stars, typically in the Magellenic Clouds, and look for an amplification of the measured light yield from these stars due to the transit of a dark brown dwarf between the Earth and the star: microlensing.

Two experiments have published results, EROS [47] and MACHO [48]. Both experiments observe microlensing events but in quantities which do not indicate a large contribution to dark matter from this source. Figure 9 shows a summary of the results interpreted assuming a galactic halo of dark matter with total mass $4 \cdot 10^{11}$ solar masses. The data from EROS excludes more than a 30% brown dwarf contribution to the halo mass fraction for masses between 10^{-7} and 1 times the solar mass whereas MACHO results allow between 10-50% halo fraction for masses around 0.5 times the solar mass. Although expressed differently these results are self-consistent as can be seen from figure 9.

14. Direct Cold Dark Matter searches

Cold dark matter searches have been reviewed at this conference by N. Spooner [49]. Direct searches for dark matter in the form of massive weakly interacting particles, WIMPs, rely on the motion of the dark matter forming the galactic halo, relative to a detector fixed on the Earth. The typical speed of a WIMP hitting a detector would be 250 km/s causing a characteristic nuclear recoil of energy ~ 10 keV in the range of WIMP masses searched for. The energy spectrum of the nuclear recoils would be an exponential with this typical characteristic energy, unfortunately similar to the form of the dominant backgrounds. The

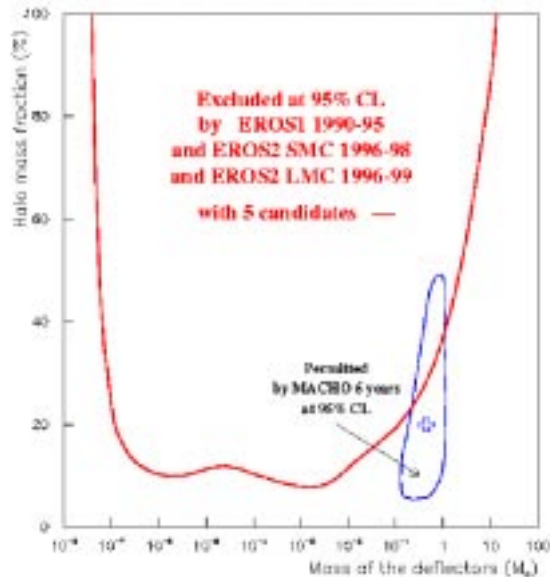


Figure 9: Results of EROS and MACHO experiments on search for Brown Dwarfs.

many experiments in the field take different approaches to distinguish the signal from the background using ionisation, scintillation, thermal and acoustic detection techniques.

A powerful tool to demonstrate a WIMP signal is to observe the modulation due to the motion of the Earth through the wind of WIMPs in the galactic halo. As the Earth orbits the sun the velocity of the Earth relative to the halo changes annually. Evidence for such a modulation has been claimed in the data of the DAMA experiment [50] using NaI detector with no background rejection which has a total exposure of ~ 60000 kg.days. Figure 10 displays this data, covering a period of 4 years, showing a modulation in the data residuals corresponding to variations of a few percent in the counting rate, in the energy range 2 to 6 keV. The data is interpreted as evidence for a WIMP with mass around $30\text{-}100$ GeV/c^2 and the contoured area in figure 11 indicates the allowed range of mass vs. cross-section from the DAMA data.

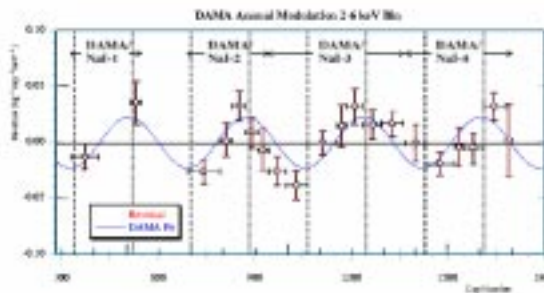


Figure 10: Data of the DAMA experiment indicating an annual modulation of counting rate in NaI detectors.

Two experiments have data that probe the region of the DAMA claim. The CDMS [51] experiment uses Si and Ge detectors with a total exposure of ~ 12 kg.days. These detectors measure both ionisation and total energy enabling an efficient rejection of background from electron events while neutron recoils from cosmic rays are indistinguishable from the signal. The CDMS experiment observes 13 recoil events which are consistent with the rate predicted for cosmic ray induced neutron events. The data is analysed making a subtraction for these neutron events and the exclusion zone shown in figure 11 is given. Using a similar detector with an exposure of ~ 5 kg.days but at a deep site protected against cosmic ray induced events, the EDELWEISS [52] experiment observes zero signal like events. Here a background subtraction is necessary and so the result is more reliable, however due to the smaller exposure the exclusion region indicated in figure 11 excludes less of the DAMA favoured zone.

If the WIMP is taken to be the neutralino from supersymmetric theory, then the lower mass limit from LEP, of 45.6 GeV/c^2 at 95%CL [53], can be added in figure 11. With all the existing data a small allowed region remains at high mass with low cross-section and so further data is required to resolve the issue.

The region of the DAMA signal will soon be fully explored with the existing generation of detectors, however to fully cover the range of cross-sections predicted for all the parameter space of the minimal supersymmetric model (MSSM) a new generation of detectors will be necessary. It is generally accepted [49] that a detector of mass 1 tonne is required and to achieve this scale of detector various research and development programs are in progress. Among the most interesting new projects are liquid Xenon detectors [49] and superheated droplet detectors [54].

15. Indirect Cold Dark Matter searches

The direct WIMP detection experiments are sensitive to any particle capable of causing a nuclear recoil while the indirect searches, described in this section, require a model as to the nature of the WIMP. Generally supersymmetric models are applied with the neutralino as the dark matter candidate particle and in the MSSM the neutralino-nucleon cross-sections can be predicted for given model parameters. These models also predict the annihilation cross-sections of neutralinos and so the rates in the various indirect searches for dark matter. Two different searches are made for neutralino annihilations; the first, annihilations occurring in the galactic halo giving gamma rays of unique energies in reaction like $\chi\chi \rightarrow Z\gamma, \gamma\gamma$ and the second, annihilations in regions of concentrations of neutralinos in massive bodies in reactions such as $\chi\chi \rightarrow WW, ff$ with W or f decaying to neutrinos.

The searches for gamma ray lines from annihilations in the halo are performed in the satellite and ground based gamma ray telescopes mentioned in section 3. In these experiments the gamma ray line energy would be directly related to the neutralino mass and give a very clear signature. The neutrino telescopes, described in section 10, search for the neutrino decay products in the annihilations in massive bodies. Concentration of neutralinos in massive bodies such as the Earth, Sun and Galactic Centre would build up since the early universe where the neutralino dark matter would naturally be a fossil of the big bang similar to the 3K relic photons. Given the matter density in the various bodies and the total dark matter content in the halo, calculations can be made as a function of MSSM parameters for the rates to be expected in the current and future experiments. The SuperKamiokande experiment has searched for high energy neutrinos from Earth, Sun and Galactic Centre and performed an analysis to set limits in the phase space of cross-section vs. mass as shown in figure 12 [55].

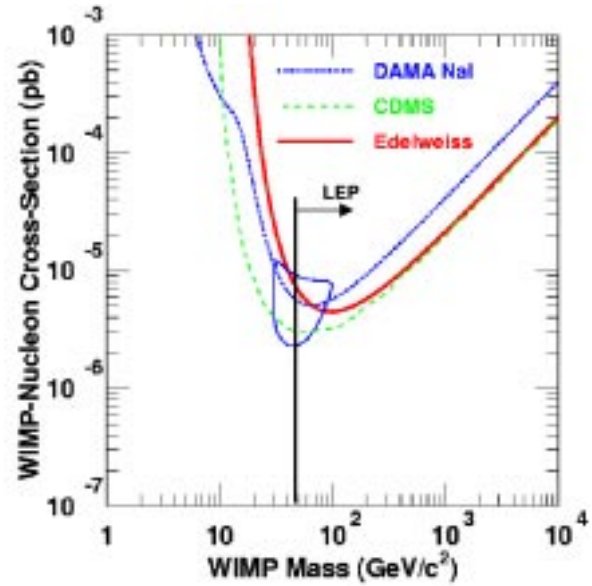


Figure 11: Results from direct searches for cold dark matter. The contour is the allowed region from the DAMA experiment. The curves are the upper limits on the cross-section from the CDMS and Edelweiss experiments as well as a limit from the DAMA experiment using pulse shape discrimination. The lower limit on the mass of the neutralino from LEP is shown.

16. Conclusions

After many decades of experiments, the nature of the sources of cosmic rays observed on Earth is still unknown. Recent data on anisotropy from AGASA start to give indications of point sources of cosmic rays at high energy and data on mass composition from KASCADE give a clue on the nature of the knee feature of the energy spectrum. The gamma ray telescope now have clearly established a few sources of TeV gammas, however, the information from these detectors still has not resolved the charged cosmic ray enigma. It is clear that new experiments are needed to continue to explore the sources of high energy radiation. Many such experiments are now under construction and as well as the new more sensitive cosmic ray and gamma detectors, it is possible that the coming new generation of neutrino telescopes will give fundamentally different information to clarify these issues.

Searches for dark matter have advanced greatly in the past few years. Hints of the existence of WIMPs have come from the DAMA experiment and have been partially refuted by the CDMS and EDELWEISS experiments. More data should soon be available to resolve this issue from all of these experiments and future, much larger, cold dark matter experiments are currently being planned. These detectors and the indirect searches possible with gamma and neutrino telescopes, will enable cold dark matter searches to extend down to much lower cross-sections and hopefully discover this missing component in the matter composition of the universe.

References

- [1] E.G. Berezhko and H.J. Volk, *Astropart. Phys.* **7** (1997) 183
- [2] M. Sikora et al., *Astrophys. J.* **421** (1994) L153
- [3] P.L. Biermann and K. Mannheim, *Astron. Astrophys.* **221** (1989) 211
- [4] I. F. Mirabel, [astro-ph/0011315](https://arxiv.org/abs/astro-ph/0011315)
- [5] <http://www-akeno.icrr.u-tokyo.ac.jp/AGASA/>
- [6] <http://www-ik.fzk.de/KASCADE-home.html>
- [7] M. Nagano and A.A.Watson, *Rev. Mod. Phys.* **72** (2000) 689
- [8] <http://egret.sao.arizona.edu>

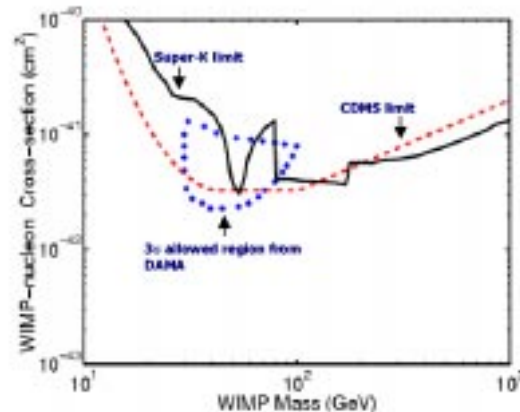


Figure 12: Results from indirect searches for cold dark matter dark from the SuperKamiokande experiment. The limit includes data searching for a neutrino signal from the centres of Earth, sun and galaxy. The allowed region from DAMA and the excluded region from CDMS are shown.

- [9] <http://www.mpi-hd.mpg.de/hfm/CT/CT.html>
- [10] D.A. Smith et al., (CELESTE Collaboration), *Nucl. Phys.* **54** (*Proc. Suppl.*) (1997) 362.
- [11] S. Oser et al., (STACEE Collaboration), *Astrophys. J.* **547** (2001) 949.
- [12] I.A. Belolaptikov et al., (BAIKAL Collaboration), *Astropart. Phys.* **7** (1997) 263.
- [13] E. Andres et al., (AMANDA Collaboration), *Nature* **410** (2001) 441.
- [14] S. Swordy, private communication.
- [15] K. Greisen., *Phys. Rev. Lett.* **16** (1966) 748, Z.T. Zapsepin and V.A. Kuzmin, *Zh. Eksp. Teor. Fiz. Pisma Red.* **4** (1966) 144.
- [16] S. Yoshida et al., *Astropart. Phys.* **3** (1995) 105.
- [17] T.K. Gaisser, [astro-ph/0011524](#).
- [18] A.D. Erlykin and A.W. Wolfendale, [astro-ph/0103477](#).
- [19] R. Wigmans, *Nucl. Phys.* **85** (*Proc. Suppl.*) (2000) 305.
- [20] M. Dova et al., [astro-ph/0112191](#).
- [21] A. M. Hillas, *Ann. Rev. Astron. & Astrophys.* **22** (1984) 425.
- [22] G. Sigl, [astro-ph/0008364](#).
- [23] M. Roth, contribution to these proceedings.
- [24] M. Takeda et al., *Astrophys. J.* **522** (1999) 225, M. Takeda et al., Proceedings of 27th ICRC, Hamburg 2001.
- [25] Y.Uchihori et al., *Astropart. Phys.* **13** (2000) 151
- [26] N. Hayashida et al., *Astropart. Phys.* **10** (1999) 303
- [27] J.A. Bellido et al., *Astropart. Phys.* **15** (2001) 167
- [28] M.T. Dova (AUGER Collaboration), Proceedings of 27th ICRC, Hamburg 2001.
- [29] W. Wallraff, these proceedings.
- [30] T. Weekes [astro-ph/0010431](#) and private communication.
- [31] J. Cortina, 'TeV gamma rays from AGNs', these proceedings
- [32] B. Funk et al., *Astropart. Phys.* **9** (1998) 97.
- [33] G. Sullivan (MILAGRO Collaboration), Proceedings of 27th ICRC, Hamburg 2001.
- [34] R. Atkins et al., (MILAGRO Collaboration), *Astrophys. J.* **533** (2000) L119.
- [35] A.J. Smith (MILAGRO Collaboration), Proceedings of 27th ICRC, Hamburg 2001: 2731.
- [36] M. Ambrosio et al., (MACRO Collaboration), *Astrophys. J.* **546** (2001) 1038, L. Perrone, Proceedings of 27th ICRC, Hamburg 2001: 1073.
- [37] V.A. Balkanov et al., (BAIKAL Collaboration), *Astropart. Phys.* **14** (2000) 61.
- [38] G.C. Hill et al., (AMANDA Collaboration) Proceedings of 27th ICRC, Hamburg 2001
- [39] M. Kowalski et al.,(AMANDA Collaboration), these proceedings.
- [40] F.W. Stecker and M.H. Salamon, [astro-ph/9501064](#).

- [41] V.S. Berezinsky et al., *Astrophysics of Cosmic Rays*, North Holland, Amsterdam (1990), K. Mannheim, R.J. Protheroe and R.J. Rachen, [astro-ph/9812398](#), E. Waxman and J.N. Bahcall, *Phys. Rev. D* **59** (1999) 023003
- [42] R. Wischnewski et al., (AMANDA Collaboration), Proceedings ICRC 2001.
- [43] <http://antares.in2p3.fr>
- [44] <http://www.nestor.org.gr>
- [45] M.S. Turner, [astro-ph/9904051](#).
- [46] L. Bergstrom, *Rep. Prog. Phys.* **63** (2000) 793, [hep-ph/0002126](#).
- [47] N. Palanque-Delabrouille et al., (EROS Collaboration), *Astron. Astrophys.* **332** (1998) 1.
- [48] C.B. Alcock et al., (MACHO Collaboration), *Astrophys. J.* **542** (2000) 281.
- [49] N. Spooner, these proceedings.
- [50] R. Bernabei et al., (DAMA Collaboration), *Phys. Lett. B* **424** (1998) 195, R. Bernabei et al., *Nucl. Phys.* **91** (*Proc. Suppl.*) (2001) 361.
- [51] R. Abusaidi et al., (CDMS Collaboration), *Phys. Rev. Lett.* **84** (2000) 5699.
- [52] A. Benoit et al., (EDELWEISS Collaboration), *Phys. Lett. B* **513** (2001) 195.
- [53] F. Gianotti, these proceedings.
- [54] N. Boukhira et al., *Astropart. Phys.* **14** (2000) 227 J.I. Collar et al., *New Jour. Phys.* **2** (2000) 14.
- [55] A. Habig et al., (SuperKamiokande Collaboration), Proceedings of 27th ICRC, Hamburg 2001, [hep-ex/0106024](#).